

DISCRETE HYPERBOLIC CURVATURE FLOW IN THE PLANE*

KLAUS DECKELNICK[†] AND ROBERT NÜRNBERG[‡]

Abstract. Hyperbolic curvature flow is a geometric evolution equation that in the plane can be viewed as the natural hyperbolic analogue of curve shortening flow. It was proposed by Gurtin and Podio-Guidugli [*SIAM J. Math. Anal.*, 22 (1991), pp. 575–586] to model certain wave phenomena in solid-liquid interfaces. We introduce a semidiscrete finite difference method for the approximation of hyperbolic curvature flow and prove error bounds for natural discrete norms. We also present numerical simulations, including the onset of singularities starting from smooth strictly convex initial data.

Key words. hyperbolic curvature flow, normal parameterization, finite differences, error analysis

MSC codes. 65M06, 65M12, 65M15, 53E10, 35L70

DOI. 10.1137/22M1493112

1. Introduction. The analytical and numerical study of parabolic geometric evolution equations, such as mean curvature flow, surface diffusion, and Willmore flow, to name a few, has received considerable attention in the literature over the last few decades; see, e.g., [19, 14, 7, 22, 21, 6, 5, 2, 8, 18, 1]. On the other hand, hyperbolic evolution laws for moving interfaces have been studied far less. In this paper, we are going to investigate the numerical approximation of the hyperbolic geometric evolution equation

$$(1.1) \quad \alpha \partial_t^\square \mathcal{V}_\Gamma + \beta \mathcal{V}_\Gamma = \varkappa_\Gamma \quad \text{on } \Gamma(t)$$

for a family of closed curves $(\Gamma(t))_{t \in [0, T]}$ in \mathbb{R}^2 . Here \mathcal{V}_Γ denotes the velocity of $(\Gamma(t))_{t \in [0, T]}$ in the direction of the normal ν_Γ , ∂_t^\square is the normal time derivative on $(\Gamma(t))_{t \in [0, T]}$, and \varkappa_Γ denotes the curvature of $\Gamma(t)$. Our sign convention is such that the unit circle with outward normal has curvature $\varkappa_\Gamma = -1$. The flow (1.1) corresponds to the evolution law proposed in [11, equation (1.2)], in the case of an isotropic surface energy and in the absence of external forcings, where it was suggested as a model for the evolution of melting-freezing waves at the solid-liquid interface of crystals such as ⁴He helium. Here the parameters $\alpha \in \mathbb{R}_{\geq 0}$ and $\beta \in \mathbb{R}_{\geq 0}$ play the role of an effective density and a kinetic coefficient, respectively. In the special case $\alpha = 1$ and $\beta = 0$, we obtain the hyperbolic geometric evolution law

$$(1.2) \quad \partial_t^\square \mathcal{V}_\Gamma = \varkappa_\Gamma \quad \text{on } \Gamma(t),$$

while the choices $\alpha = 0$ and $\beta = 1$ yield the well-known (mean) curvature flow, or curve shortening flow. However, since in this work we are interested in the hyperbolic case, we shall from now on set $\alpha = 1$ for simplicity. We remark that in order to close the geometric evolution equation (1.1), the initial conditions

*Received by the editors April 27, 2022; accepted for publication (in revised form) March 27, 2023; published electronically July 20, 2023.

<https://doi.org/10.1137/22M1493112>

[†]Institut für Analysis und Numerik, Otto-von-Guericke-Universität Magdeburg, 39106 Magdeburg, Germany (klaus.deckelnick@ovgu.de).

[‡]Dipartimento di Matematica, Università di Trento, 38123 Trento, Italy (robert.nurnberg@unitn.it).

$$\Gamma(0) = \Gamma_0 \quad \text{and} \quad \mathcal{V}_\Gamma|_{t=0} = \mathcal{V}_{\Gamma,0}$$

need to be prescribed, where Γ_0 defines the initial curve and $\mathcal{V}_{\Gamma,0} : \Gamma_0 \rightarrow \mathbb{R}$ gives an initial normal velocity.

Let us consider a parametric description of the evolving curves, i.e., $\Gamma(t) = x(I, t)$ for some mapping $x : I \times [0, T] \rightarrow \mathbb{R}^2$, where $I = \mathbb{R}/\mathbb{Z}$ is the periodic interval $[0, 1]$. We denote by

$$(1.3) \quad \tau = \frac{x_\rho}{|x_\rho|}, \quad \nu = \tau^\perp = \frac{x_\rho^\perp}{|x_\rho|}, \quad \text{and} \quad \varkappa\nu = \frac{\tau_\rho}{|x_\rho|} = \frac{1}{|x_\rho|} \left(\frac{x_\rho}{|x_\rho|} \right)_\rho$$

the unit tangent, the unit normal, and the curvature vector, respectively, so that, e.g., $\nu = \nu_\Gamma \circ x$ and $\varkappa = \varkappa_\Gamma \circ x$. Here and throughout, \cdot^\perp denotes the anticlockwise rotation through $\frac{\pi}{2}$. We shall show in Lemma 2.1 below that if x is a solution of the system

$$(1.4a) \quad x_{tt} + \beta x_t = \frac{1}{|x_\rho|} \left(\frac{x_\rho}{|x_\rho|} \right)_\rho - (x_t \cdot \tau_t) \tau \quad \text{in } I \times (0, T],$$

$$(1.4b) \quad x(\cdot, 0) = x_0, \quad x_t(\cdot, 0) = \mathcal{V}_0 \nu(\cdot, 0) \quad \text{in } I,$$

then the curves $(\Gamma(t))_{t \in [0, T]}$ evolve according to (1.1) with $\alpha = 1$. In the above, $x_0 : I \rightarrow \mathbb{R}^2$ is a parameterization of the given initial curve Γ_0 and $\mathcal{V}_0 = \mathcal{V}_{\Gamma,0} \circ x_0$ is induced by the given initial normal velocity $\mathcal{V}_{\Gamma,0}$. The introduction of the second term on the right-hand side of (1.4a) has the effect that the parameterization x is normal, i.e., it satisfies $x_t \cdot \tau = 0$; see also Lemma 2.1. The system (1.4) in the case $\beta = 0$ has been studied in [15, 16]; see also [12]. In particular, it is shown in [15] that if $\Gamma(0)$ is strictly convex, and if the initial velocity $\mathcal{V}_0 \nu(\cdot, 0)$ does not point outwards anywhere on $\Gamma(0)$, then the solution to (1.4) exists on a finite time interval $[0, T_{\max})$ and the curves $\Gamma(t)$ remain strictly convex. Furthermore, as $t \rightarrow T_{\max}$, $\Gamma(t)$ either shrinks to a point or converges to a convex curve with discontinuous curvature.

One may wonder whether it is possible to replace (1.4a) by the simpler hyperbolic equation

$$(1.5) \quad x_{tt} = \frac{1}{|x_\rho|} \left(\frac{x_\rho}{|x_\rho|} \right)_\rho \quad \text{in } I \times (0, T],$$

which has been considered in, e.g., [13] after having been proposed by Yau in [23, p. 242]. However, in contrast to (1.4), it is not clear whether solutions to (1.5) with the initial conditions (1.4b) parameterize solutions to the flow (1.2). In fact, numerical evidence in section 5.4, below, suggests that solutions to (1.4) and (1.5), (1.4b) parameterize different curve evolutions.

An alternative hyperbolic geometric evolution equation that is similar to (1.4) and which has been considered in [17] is described by

$$(1.6) \quad x_{tt} = \frac{1}{2}(|x_t|^2 + 1) \frac{1}{|x_\rho|} \left(\frac{x_\rho}{|x_\rho|} \right)_\rho - (x_t \cdot \tau_t) \tau \quad \text{in } I \times (0, T],$$

$$x(\cdot, 0) = x_0, \quad x_t(\cdot, 0) = \mathcal{V}_0 \nu(\cdot, 0) \quad \text{in } I.$$

It can be shown that solutions to (1.6) also represent normal parameterizations of curves. An interesting aspect of (1.6) in terms of the analysis is that its solutions satisfy the energy conservation

$$\frac{1}{2} \frac{d}{dt} \int_I (|x_t|^2 + 1) |x_\rho| \, d\rho = 0.$$

In contrast, for the flow (1.4) a conditional decay property can be shown for the energy $\frac{1}{2} \int_I (|x_t|^2 + 2)|x_\rho| \, d\rho$ (see Remark 2.2 below), something that we will utilize for the numerical analysis presented in this paper. Let us finally mention that geometric second order hyperbolic PDEs have recently been used in [3] for applications in image processing.

As regards the numerical approximation of hyperbolic geometric evolution equations in the literature, we are only aware of the works [20, 9]. In the former, an algorithm for the evolution of polygonal curves under crystalline hyperbolic curvature flow is presented, which corresponds to (1.1) for a crystalline, anisotropic surface energy. On the other hand, in [9] a level-set approach, which is based on a threshold algorithm of BMO type, is used for the numerical solution of (1.5).

In this paper, we will present a finite difference approximation of (1.4) and prove an error bound for it. To the best of our knowledge, this is the first result on the numerical analysis for a hyperbolic geometric evolution equation in the literature.

The remainder of the paper is organized as follows. In section 2, we show that curves $\Gamma(t)$ that are parameterized by solutions of (1.4) evolve according to (1.1). We also derive several properties of these solutions. In section 3, we introduce our semidiscrete finite difference approximation and state our main result, Theorem 3.5. Its proof is presented in section 4. Finally, in section 5 we suggest a fully discrete scheme and present several numerical simulations for it, including a convergence experiment and simulations that lead to nonvanishing singularities in finite time.

2. Mathematical formulation. Consider a family $(\Gamma(t))_{t \in [0, T]}$ of evolving curves that are given by $\Gamma(t) = x(I, t)$, where $x : I \times [0, T] \rightarrow \mathbb{R}^2$ satisfies $|x_\rho| > 0$ in $I \times [0, T]$. Then the unit normal on Γ , the curvature of Γ , and the normal velocity of Γ , as well as the normal time derivative on Γ , are defined by the following identities in I (see, e.g., [1]):

$$(2.1) \quad \nu_\Gamma \circ x = \nu, \quad \varkappa_\Gamma \circ x = \varkappa, \quad \mathcal{V}_\Gamma \circ x = x_t \cdot \nu, \quad (\partial_t^\square f) \circ x = (f \circ x)_t - (f \circ x)_s x_t \cdot \tau,$$

where $\partial_s = |x_\rho|^{-1} \partial_\rho$ denotes differentiation with respect to arclength s . We stress that the definitions of the above quantities are independent of the chosen parameterization. The following lemma establishes the connection to the evolution law (1.1) and derives additional properties of x that will be useful in the subsequent analysis.

LEMMA 2.1. *Suppose that $x : I \times [0, T] \rightarrow \mathbb{R}^2$ is a solution of (1.4). Then the curves $(\Gamma(t))_{t \in [0, T]}$ with $\Gamma(t) = x(I, t)$ evolve according to (1.1). Furthermore, x is a normal parameterization, i.e.,*

$$(2.2) \quad x_t \cdot \tau = 0 \quad \text{in } I \times [0, T],$$

and satisfies

$$(2.3) \quad \partial_t |x_\rho| = -|x_\rho| x_t \cdot x_{tt} - \beta |x_\rho| |x_t|^2 \quad \text{in } I \times [0, T].$$

Proof. Using (1.4a) and (1.3) we deduce that

$$(x_t \cdot \tau)_t = x_{tt} \cdot \tau + x_t \cdot \tau_t = (\varkappa \nu - (x_t \cdot \tau_t) \tau - \beta x_t) \cdot \tau + x_t \cdot \tau_t = -\beta x_t \cdot \tau.$$

In view of (1.4b), we have $(x_t \cdot \tau)|_{t=0} = 0$, which implies (2.2). With the help of (2.1) and (2.2) we now deduce

$$\begin{aligned} (\partial_t^\square \mathcal{V}_\Gamma) \circ x + \beta \mathcal{V}_\Gamma \circ x &= [(x_t \cdot \nu)_t - (x_t \cdot \nu)_s x_t \cdot \tau] + \beta x_t \cdot \nu \\ &= x_{tt} \cdot \nu + x_t \cdot \nu_t + \beta x_t \cdot \nu = x_{tt} \cdot \nu + \beta x_t \cdot \nu \\ &= \varkappa \nu \cdot \nu = \varkappa = \varkappa_\Gamma \circ x \quad \text{in } I \times [0, T], \end{aligned}$$

where we used that $0 = \frac{1}{2}(|\nu|^2)_t = \nu_t \cdot \nu$, (1.3), and (1.4a). Thus, (1.1) holds on $\Gamma(t)$. Finally, recalling again (2.2) and (1.4a), we obtain

$$(2.4) \quad \partial_t |x_\rho| = x_{t\rho} \cdot \tau = -x_t \cdot \tau_\rho = -|x_\rho| x_t \cdot x_{tt} - \beta |x_\rho| |x_t|^2 \quad \text{in } I \times [0, T],$$

which proves (2.3). \square

Remark 2.2. Using (2.4) and (2.2) we derive the following energy law:

$$\begin{aligned} (2.5) \quad \frac{1}{2} \frac{d}{dt} \int_I (|x_t|^2 + 2)|x_\rho| \, d\rho &= \frac{1}{2} \int_I |x_t|^2 \partial_t |x_\rho| \, d\rho + \int_I x_t \cdot x_{tt} |x_\rho| + \partial_t |x_\rho| \, d\rho \\ &= -\frac{1}{2} \int_I |x_t|^2 x_t \cdot \tau_\rho \, d\rho - \beta \int_I |x_t|^2 |x_\rho| \, d\rho \\ &= -\frac{1}{2} \int_I (x_t \cdot \nu)^3 \varkappa |x_\rho| \, d\rho - \beta \int_I (x_t \cdot \nu)^2 |x_\rho| \, d\rho, \end{aligned}$$

which corresponds to [11, equation (4.6)] in the absence of external forces. An adaptation of this relation to the error between continuous and discrete solution will be at the heart of our error analysis.

For the remainder of the paper, we make the following regularity assumptions concerning the solution x .

Assumption 2.3. $x : I \times [0, T] \rightarrow \mathbb{R}^2$ is a solution of (1.4) such that $\partial_t^i \partial_\rho^j x$ exist and are continuous on $I \times [0, T]$ for all $i, j \in \mathbb{N} \cup \{0\}$ with $2i + j \leq 4$. Furthermore, $|x_\rho| > 0$ in $I \times [0, T]$.

Assumption 2.3 implies in particular that there exist constants $0 < c_0 \leq C_0$ such that

$$(2.6) \quad c_0 \leq |x_\rho| \leq C_0 \quad \text{in } I \times [0, T], \quad \max_{I \times [0, T]} (|\tau_\rho| + |x_t| + |x_{t\rho}|) \leq C_0.$$

3. Finite difference discretization. We shall employ a finite difference scheme in order to discretize (1.4) in space. To do so, let us introduce the set of grid points $\mathcal{G}^h := \{\rho_1, \dots, \rho_J\} \subset I$, where $\rho_j = jh$, $j = 0, \dots, J$, and $h = \frac{1}{J}$ for $J \geq 2$. In order to account for our periodic setting, we always identify ρ_0 with ρ_J . For a grid function $v : \mathcal{G}^h \rightarrow \mathbb{R}^2$, we write $v_j := v(\rho_j)$, $j = 1, \dots, J$, and in addition set $v_0 = v_J$ and $v_{J+1} = v_1$ in view of the periodicity of I . We associate with v the backward difference quotient

$$(3.1) \quad \delta v_j := \frac{v_j - v_{j-1}}{h}, \quad j = 1, \dots, J,$$

and introduce the following discrete norms:

$$(3.2) \quad \|v\|_{0,h} := \left(h \sum_{j=1}^J |v_j|^2 \right)^{\frac{1}{2}}, \quad \|v\|_{1,h} := \left(h \sum_{j=1}^J (|v_j|^2 + |\delta v_j|^2) \right)^{\frac{1}{2}}.$$

Let $x^h : \mathcal{G}^h \rightarrow \mathbb{R}^2$ be a grid function that will play the role of a discrete parameterization of a curve. Then on $I_j = [\rho_{j-1}, \rho_j]$ the associated discrete length element q_j^h and the discrete tangent τ_j^h are given by

$$q_j^h = |\delta x_j^h|, \quad \tau_j^h = \frac{1}{q_j^h} \delta x_j^h, \quad j = 1, \dots, J.$$

It will be convenient to also introduce the averaged vertex tangent θ_j^h via

$$(3.3) \quad \theta_j^h = \frac{\tau_j^h + \tau_{j+1}^h}{|\tau_j^h + \tau_{j+1}^h|}, \quad \text{provided that } \tau_j^h + \tau_{j+1}^h \neq 0, \quad j = 1, \dots, J.$$

Clearly,

$$(3.4) \quad (\tau_{j+1}^h - \tau_j^h) \cdot \theta_j^h = (\tau_{j+1}^h - \tau_j^h) \cdot \frac{\tau_j^h + \tau_{j+1}^h}{|\tau_j^h + \tau_{j+1}^h|} = \frac{1}{|\tau_j^h + \tau_{j+1}^h|} (|\tau_{j+1}^h|^2 - |\tau_j^h|^2) = 0.$$

LEMMA 3.1. *Let $x \in C^4(I; \mathbb{R}^2)$ such that $c_0 \leq |x_\rho| \leq C_0$ in I , and set $\tau = \frac{x_\rho}{|x_\rho|}$ as well as*

$$x_j = x(\rho_j), \quad q_j = |\delta x_j| \quad \text{and} \quad \tau_j = \frac{1}{q_j} \delta x_j, \quad j = 1, \dots, J.$$

Then there exists $h_* > 0$ such that for all $0 < h \leq h_*$ and all $j = 1, \dots, J$ we have

$$(3.5) \quad \frac{1}{2} c_0 \leq q_j \leq 2C_0$$

and

$$(3.6a) \quad \frac{1}{2}(q_j + q_{j+1}) = |x_\rho(\rho_j)| + \mathcal{O}(h^2);$$

$$(3.6b) \quad \tau_j + \tau_{j+1} = 2\tau(\rho_j) + \mathcal{O}(h^2);$$

$$(3.6c) \quad \frac{\tau_{j+1} - \tau_j}{h} = \tau_\rho(\rho_j) + \mathcal{O}(h^2).$$

Proof. A Taylor expansion yields

$$\delta x_{j+1} = \frac{x_{j+1} - x_j}{h} = x_\rho + \frac{h}{2} x_{\rho\rho} + \frac{h^2}{6} x_{\rho\rho\rho} + \mathcal{O}(h^3),$$

where all the derivatives of x , and τ , in this proof are evaluated at ρ_j . Hence,

$$\begin{aligned} q_{j+1}^2 &= |x_\rho|^2 + h x_{\rho\rho} \cdot x_\rho + \frac{h^2}{4} |x_{\rho\rho}|^2 + \frac{h^2}{3} x_{\rho\rho\rho} \cdot x_\rho + \mathcal{O}(h^3) \\ &= |x_\rho|^2 \left(1 + h \frac{x_{\rho\rho}}{|x_\rho|} \cdot \tau + h^2 \left[\frac{1}{4} \frac{|x_{\rho\rho}|^2}{|x_\rho|^2} + \frac{1}{3} \frac{x_{\rho\rho\rho}}{|x_\rho|} \cdot \tau \right] + \mathcal{O}(h^3) \right), \end{aligned}$$

and with $\sqrt{1 + \varepsilon} = 1 + \frac{1}{2}\varepsilon - \frac{1}{8}\varepsilon^2 + \mathcal{O}(\varepsilon^3)$ it therefore follows that

$$q_{j+1} = |x_\rho| \left(1 + \frac{h}{2} \frac{x_{\rho\rho}}{|x_\rho|} \cdot \tau + h^2 \left[\frac{1}{8} \frac{|x_{\rho\rho}|^2}{|x_\rho|^2} + \frac{1}{6} \frac{x_{\rho\rho\rho}}{|x_\rho|} \cdot \tau - \frac{1}{8} \frac{(x_{\rho\rho} \cdot \tau)^2}{|x_\rho|^2} \right] \right) + \mathcal{O}(h^3).$$

Moreover, since $\tau_{j+1} = \frac{1}{q_{j+1}} \delta x_{j+1}$ and $\frac{1}{1 + \varepsilon} = 1 - \varepsilon + \varepsilon^2 + \mathcal{O}(\varepsilon^3)$, we have that

$$\begin{aligned} \tau_{j+1} &= \tau + \frac{h}{2} \tau_\rho + h^2 \left[\frac{1}{6} \frac{x_{\rho\rho\rho}}{|x_\rho|} - \left[\frac{1}{8} \frac{|x_{\rho\rho}|^2}{|x_\rho|^2} + \frac{1}{6} \frac{x_{\rho\rho\rho}}{|x_\rho|} \cdot \tau - \frac{3}{8} \frac{(x_{\rho\rho} \cdot \tau)^2}{|x_\rho|^2} \right] \tau - \frac{1}{4} \left(\frac{x_{\rho\rho}}{|x_\rho|} \cdot \tau \right) \frac{x_{\rho\rho}}{|x_\rho|} \right] \\ &\quad + \mathcal{O}(h^3), \end{aligned}$$

where we used that $\frac{x_{\rho\rho}}{|x_\rho|} - (\frac{x_{\rho\rho}}{|x_\rho|} \cdot \tau)\tau = (\frac{x_\rho}{|x_\rho|})_\rho = \tau_\rho$. In a similar way, one finds that

$$q_j = |x_\rho| \left(1 - \frac{h}{2} \frac{x_{\rho\rho}}{|x_\rho|} \cdot \tau + h^2 \left[\frac{1}{8} \frac{|x_{\rho\rho}|^2}{|x_\rho|^2} + \frac{1}{6} \frac{x_{\rho\rho\rho}}{|x_\rho|} \cdot \tau - \frac{1}{8} \frac{(x_{\rho\rho} \cdot \tau)^2}{|x_\rho|^2} \right] \right) + \mathcal{O}(h^3);$$

$$\tau_j = \tau - \frac{h}{2} \tau_\rho + h^2 \left[\frac{1}{6} \frac{x_{\rho\rho\rho}}{|x_\rho|} - \left[\frac{1}{8} \frac{|x_{\rho\rho}|^2}{|x_\rho|^2} + \frac{1}{6} \frac{x_{\rho\rho\rho}}{|x_\rho|} \cdot \tau - \frac{3}{8} \frac{(x_{\rho\rho} \cdot \tau)^2}{|x_\rho|^2} \right] \tau - \frac{1}{4} \left(\frac{x_{\rho\rho}}{|x_\rho|} \cdot \tau \right) \frac{x_{\rho\rho}}{|x_\rho|} \right] + \mathcal{O}(h^3).$$

From the above we infer that (3.5) holds provided that $0 < h \leq h_*$. The estimates (3.6) also follow immediately. \square

In view of (3.6a), a natural semidiscrete finite difference approximation of (1.4) is now defined as follows. Find $x^h : \mathcal{G}^h \times [0, T] \rightarrow \mathbb{R}^2$ such that

$$(3.7a) \quad \ddot{x}_j^h + \beta \dot{x}_j^h = \frac{2}{q_j^h + q_{j+1}^h} \frac{\tau_{j+1}^h - \tau_j^h}{h} - (\dot{x}_j^h \cdot \dot{\theta}_j^h) \theta_j^h \quad \text{in } [0, T], \quad j = 1, \dots, J;$$

$$(3.7b) \quad x_j^h(0) = x_0(\rho_j), \quad \dot{x}_j^h(0) = \mathcal{V}_0(\rho_j) \theta_j^{h,\perp}(0), \quad j = 1, \dots, J.$$

Standard ODE theory implies that the above system has a unique solution on some interval $[0, T_h)$. Let us begin by deriving discrete analogues of (2.2) and (2.3).

LEMMA 3.2. *Let $x^h : \mathcal{G}^h \times [0, T_h) \rightarrow \mathbb{R}^2$ be a solution of (3.7). Then we have in $[0, T_h)$ and for all $j = 1, \dots, J$ that*

$$(3.8a) \quad \dot{x}_j^h \cdot \theta_j^h = 0;$$

$$(3.8b) \quad \dot{q}_j^h + \frac{1}{4}(q_{j-1}^h + q_j^h)(\dot{x}_{j-1}^h \cdot \ddot{x}_{j-1}^h + \beta |\dot{x}_{j-1}^h|^2) + \frac{1}{4}(q_j^h + q_{j+1}^h)(\dot{x}_j^h \cdot \ddot{x}_j^h + \beta |\dot{x}_j^h|^2) = 0.$$

Proof. It follows from (3.7a), (3.4), and the fact that $|\theta_j^h| = 1$ that

$$(\dot{x}_j^h \cdot \theta_j^h)_t = \ddot{x}_j^h \cdot \theta_j^h + \dot{x}_j^h \cdot \dot{\theta}_j^h = -\beta \dot{x}_j^h \cdot \theta_j^h, \quad j = 1, \dots, J.$$

Since $\dot{x}_j^h(0) \cdot \theta_j^h(0) = 0$ by (3.7b), we deduce (3.8a). In particular, $\dot{x}_j^h \cdot \tau_j^h = -\dot{x}_j^h \cdot \tau_{j+1}^h$ and hence

$$\begin{aligned} \dot{q}_j^h &= \frac{\dot{x}_j^h - \dot{x}_{j-1}^h}{h} \cdot \tau_j^h = -\frac{1}{2} \dot{x}_j^h \cdot \frac{\tau_{j+1}^h - \tau_j^h}{h} - \frac{1}{2} \dot{x}_{j-1}^h \cdot \frac{\tau_j^h - \tau_{j-1}^h}{h} \\ &= -\frac{1}{4}(q_j^h + q_{j+1}^h)(\dot{x}_j^h \cdot \ddot{x}_j^h + \beta |\dot{x}_j^h|^2) - \frac{1}{4}(q_{j-1}^h + q_j^h)(\dot{x}_{j-1}^h \cdot \ddot{x}_{j-1}^h + \beta |\dot{x}_{j-1}^h|^2), \end{aligned}$$

where the last equation is a consequence of (3.7a) and (3.8a). This proves (3.8b). \square

We also have the following discrete analogue of Remark 2.2, where for simplicity we consider only the case $\beta = 0$.

LEMMA 3.3. *Let $x^h : \mathcal{G}^h \times [0, T_h) \rightarrow \mathbb{R}^2$ be a solution of (3.7) with $\beta = 0$. Then we have in $[0, T_h)$ that*

$$(3.9) \quad \frac{1}{2} \frac{d}{dt} h \sum_{j=1}^J \left[\frac{1}{2}(q_j^h + q_{j+1}^h) |\dot{x}_j^h|^2 + 2q_j^h \right] = \frac{1}{2} h \sum_{j=1}^J \dot{q}_j^h \frac{1}{2} (|\dot{x}_{j-1}^h|^2 + |\dot{x}_j^h|^2),$$

with \dot{q}_j^h satisfying (3.8b).

Proof. We compute, on noting (3.7a) and (3.8a), that

$$\begin{aligned} \frac{1}{2} \frac{d}{dt} h \sum_{j=1}^J \frac{1}{2} (q_j^h + q_{j+1}^h) |\dot{x}_j^h|^2 &= \frac{1}{2} h \sum_{j=1}^J \frac{1}{2} (\dot{q}_j^h + \dot{q}_{j+1}^h) |\dot{x}_j^h|^2 + h \sum_{j=1}^J \frac{1}{2} (q_j^h + q_{j+1}^h) \dot{x}_j^h \cdot \ddot{x}_j^h \\ &= \frac{1}{2} h \sum_{j=1}^J \dot{q}_j^h \frac{1}{2} (|\dot{x}_{j-1}^h|^2 + |\dot{x}_j^h|^2) + h \sum_{j=1}^J \dot{x}_j^h \cdot \frac{\tau_{j+1}^h - \tau_j^h}{h} \\ &= \frac{1}{2} h \sum_{j=1}^J \dot{q}_j^h \frac{1}{2} (|\dot{x}_{j-1}^h|^2 + |\dot{x}_j^h|^2) - h \sum_{j=1}^J \frac{\dot{x}_j^h - \dot{x}_{j-1}^h}{h} \cdot \tau_j^h \\ &= \frac{1}{2} h \sum_{j=1}^J \dot{q}_j^h \frac{1}{2} (|\dot{x}_{j-1}^h|^2 + |\dot{x}_j^h|^2) - \frac{d}{dt} h \sum_{j=1}^J q_j^h, \end{aligned}$$

which is the desired result (3.9). □

Observe that the right-hand side of (3.9), in view of (3.8b), approximates the expression

$$(3.10) \quad -\frac{1}{2} \int_I |x_\rho| (x_t \cdot x_{tt}) |x_t|^2 d\rho = -\frac{1}{2} \int_I |x_\rho| (\varkappa x_t \cdot \nu) |x_t|^2 d\rho,$$

where we have noted (1.4a), (1.3), and (2.2). As (3.10) agrees with the right-hand side in (2.5) with $\beta = 0$ (recall again (2.2)), Lemma 3.3 can be viewed as a discrete analogue of Remark 2.2.

We stress that utilizing a suitable variant of (3.9) will be at the heart of our error analysis in section 4. In particular, \dot{x}_j^h will be replaced by the time derivative of the error between x and x^h at the point ρ_j ; see (4.4) below for the precise details.

Let us next consider the consistency errors for the scheme (3.7a) and for the property (3.8b).

LEMMA 3.4. *Let x be the solution of (1.4). Define*

$$(3.11a) \quad R_j := \ddot{x}_j + \beta \dot{x}_j - \frac{2}{q_j + q_{j+1}} \frac{\tau_{j+1} - \tau_j}{h} + (\dot{x}_j \cdot \tau_t(\rho_j, \cdot)) \tau(\rho_j, \cdot);$$

$$(3.11b) \quad \tilde{R}_j := \dot{q}_j + \frac{1}{4} (q_{j-1} + q_j) (\dot{x}_{j-1} \cdot \ddot{x}_{j-1} + \beta |\dot{x}_{j-1}|^2) + \frac{1}{4} (q_j + q_{j+1}) (\dot{x}_j \cdot \ddot{x}_j + \beta |\dot{x}_j|^2).$$

Then there exists a constant C_1 such that

$$(3.12) \quad \max_{j=1, \dots, J} (|R_j(t)| + |\tilde{R}_j(t)|) \leq C_1 h^2, \quad t \in [0, T].$$

Proof. The bound on R_j is a direct consequence of Lemma 3.1. In order to analyze \tilde{R}_j , we deduce from (3.6c) that $\tau_{j\pm 1} = \tau_j \pm h \tau_\rho(\rho_j, \cdot) + \mathcal{O}(h^2)$, and hence by (3.6b)

$$\tau_j = \frac{1}{2} \frac{\tau_j + \tau_{j+1}}{2} + \frac{1}{2} \frac{\tau_{j-1} + \tau_j}{2} + \mathcal{O}(h^2) = \frac{1}{2} (\tau(\rho_j, \cdot) + \tau(\rho_{j-1}, \cdot)) + \mathcal{O}(h^2).$$

Combining this relation with the fact that

$$\frac{\dot{x}_j - \dot{x}_{j-1}}{h} = \frac{1}{2} (x_{t\rho}(\rho_{j-1}, \cdot) + x_{t\rho}(\rho_j, \cdot)) + \mathcal{O}(h^2),$$

we obtain

$$\begin{aligned} \dot{q}_j &= \frac{\dot{x}_j - \dot{x}_{j-1}}{h} \cdot \tau_j = \frac{1}{4} (x_{t\rho}(\rho_{j-1}, \cdot) + x_{t\rho}(\rho_j, \cdot)) \cdot (\tau(\rho_{j-1}, \cdot) + \tau(\rho_j, \cdot)) + \mathcal{O}(h^2) \\ &= \frac{1}{2} x_{t\rho}(\rho_{j-1}, \cdot) \cdot \tau(\rho_{j-1}, \cdot) + \frac{1}{2} x_{t\rho}(\rho_j, \cdot) \cdot \tau(\rho_j, \cdot) \\ &\quad - \frac{1}{4} (x_{t\rho}(\rho_j, \cdot) - x_{t\rho}(\rho_{j-1}, \cdot)) \cdot (\tau(\rho_j, \cdot) - \tau(\rho_{j-1}, \cdot)) + \mathcal{O}(h^2) \\ &= \frac{1}{2} x_{t\rho}(\rho_{j-1}, \cdot) \cdot \tau(\rho_{j-1}, \cdot) + \frac{1}{2} x_{t\rho}(\rho_j, \cdot) \cdot \tau(\rho_j, \cdot) + \mathcal{O}(h^2) \\ &= -\frac{1}{2} |x_\rho(\rho_{j-1}, \cdot)| (\dot{x}_{j-1} \cdot \ddot{x}_{j-1} + \beta |\dot{x}_{j-1}|^2) - \frac{1}{2} |x_\rho(\rho_j, \cdot)| (\dot{x}_j \cdot \ddot{x}_j + \beta |\dot{x}_j|^2) + \mathcal{O}(h^2), \end{aligned}$$

where we have used (2.3). Now the bound on \tilde{R}_j follows with the help of (3.6a). \square

In view of Lemma 3.4, we expect second order convergence for our scheme. As our main result we prove that this is indeed the case, where the error is measured in discrete integral norms that are natural for a second order system of hyperbolic PDEs.

THEOREM 3.5. *Suppose that Assumption 2.3 is satisfied. Then there exists $h_0 > 0$ such that for $0 < h \leq h_0$ the problem (3.7) has a unique solution $x^h : \mathcal{G}^h \times [0, T] \rightarrow \mathbb{R}^2$ and the following error bounds hold:*

$$(3.13) \quad \max_{0 \leq t \leq T} (\|x(t) - x^h(t)\|_{1,h} + \|\dot{x}(t) - \dot{x}^h(t)\|_{0,h}) \leq Ch^2.$$

Here, and throughout, C denotes a generic positive constant independent of the mesh parameter h .

4. Proof of Theorem 3.5.

Let us abbreviate

$$x_j(t) = x(\rho_j, t), \quad q_j(t) = |\delta x_j(t)|, \quad \text{and} \quad \tau_j(t) = \frac{1}{q_j(t)} \delta x_j(t), \quad j = 1, \dots, J,$$

where x denotes the solution of (1.4). Furthermore, we let

$$(4.1) \quad \hat{T}_h = \sup \left\{ \hat{t} \in [0, T] : x^h \text{ solves (3.7) on } [0, \hat{t}], \text{ with } \frac{1}{4} c_0 \leq q_j^h(t) \leq 4C_0 \text{ and} \right. \\ \left. \max_{j=1, \dots, J} (|\tau_j(t) - \tau_j^h(t)| + |\dot{x}_j(t) - \dot{x}_j^h(t)|) \leq h^{\frac{5}{4}} \text{ for } 0 \leq t \leq \hat{t} \right\}.$$

Here we have chosen the power $h^{\frac{5}{4}}$ in the definition (4.1) as a convenient value between 1 and $\frac{3}{2}$, where the latter power of h arises in the proof due to the application of an inverse inequality; see (4.21) below.

Clearly, $\hat{T}_h > 0$. In view of (2.6) and Lemma 3.1 we may assume that

$$(4.2a) \quad |\tau_j + \tau_{j+1}| \geq 1$$

and hence

$$(4.2b) \quad |\tau_j^h + \tau_{j+1}^h| \geq |\tau_j + \tau_{j+1}| - |\tau_j^h - \tau_j| - |\tau_{j+1}^h - \tau_{j+1}| \geq 1 - 2h^{\frac{5}{4}} \geq \frac{1}{2},$$

provided that $0 < h \leq h_*$ is sufficiently small. Thus, $\theta_j^h(t)$ is well defined for $j = 1, \dots, J$ and $t \in [0, \hat{T}_h)$. Furthermore, we have the following lemma.

LEMMA 4.1. *There exist $0 < h_0 \leq h_*$ and a constant C_2 , which only depends on c_0, C_0 , and β , such that for all $0 < h \leq h_0$ and $0 \leq t < \hat{T}_h$*

$$\max_{j=1, \dots, J} (|\dot{x}_j^h(t)| + |\dot{\theta}_j^h(t)| + |\dot{x}_j^h(t)| + |\dot{q}_j^h(t)|) \leq C_2.$$

Proof. To begin, we deduce from (2.6) and (4.1) that

$$|\dot{x}_j^h(t)| \leq |x_t(\rho_j, t)| + |(\dot{x}_j - \dot{x}_j^h)(t)| \leq C_0 + h^{\frac{5}{4}} \leq 2C_0,$$

provided that $0 < h \leq h_0$ with h_0 sufficiently small. Next, a straightforward calculation shows that $\dot{\tau}_j^h = \frac{1}{q_j^h} (\delta \dot{x}_j^h - (\delta \dot{x}_j^h \cdot \tau_j^h) \tau_j^h)$, and hence, on noting (4.1), (3.1), and (2.6), it holds that

$$\begin{aligned} |\dot{\tau}_j^h(t)| &\leq \frac{1}{q_j^h(t)} |\delta \dot{x}_j^h(t)| \leq \frac{4}{c_0} (|\delta(\dot{x}_j^h - \dot{x}_j)(t)| + |\delta \dot{x}_j(t)|) \\ &\leq \frac{8}{c_0} \frac{1}{h} \max_{1 \leq k \leq J} |(\dot{x}_k^h - \dot{x}_k)(t)| + \frac{4}{c_0} \max_{\rho \in I} |x_{t\rho}(\rho, t)| \leq \frac{8}{c_0} h^{\frac{1}{4}} + \frac{4}{c_0} C_0 \leq \frac{8C_0}{c_0}, \end{aligned}$$

provided that $0 < h \leq h_0$ with h_0 sufficiently small. From this we deduce, on recalling (3.3) and (4.2b), that

$$|\dot{\theta}_j^h(t)| \leq \frac{|\dot{\tau}_j^h(t) + \dot{\tau}_{j+1}^h(t)|}{|\tau_j^h(t) + \tau_{j+1}^h(t)|} \leq 2 \frac{16C_0}{c_0} = \frac{32C_0}{c_0}.$$

In order to bound \ddot{x}_j^h , we first use (3.6c), (2.6), and (4.1) to show that

$$\left| \frac{\tau_{j+1}^h(t) - \tau_j^h(t)}{h} \right| \leq \left| \frac{\tau_{j+1}(t) - \tau_j(t)}{h} \right| + \frac{2}{h} \max_{k=1, \dots, J} |\tau_k(t) - \tau_k^h(t)| \leq 2C_0 + 2h^{\frac{1}{4}} \leq 3C_0,$$

provided that $0 < h \leq h_0$ with $h_0 \leq h_*$ sufficiently small. If we combine this estimate with (3.7a), (4.1), and the previously derived bounds on \dot{x}_j^h and $\dot{\theta}_j^h$, we obtain

$$\begin{aligned} |\ddot{x}_j^h(t)| &\leq \beta |\dot{x}_j^h(t)| + \frac{2}{q_j^h(t) + q_{j+1}^h(t)} \left| \frac{\tau_{j+1}^h(t) - \tau_j^h(t)}{h} \right| + |\dot{x}_j^h(t)| |\dot{\theta}_j^h(t)| \\ &\leq 2\beta C_0 + \frac{4}{c_0} 3C_0 + 2C_0 \frac{32C_0}{c_0} = 2\beta C_0 + \frac{12C_0}{c_0} + \frac{64C_0^2}{c_0}. \end{aligned}$$

Finally, the bound on \ddot{q}_j^h is a consequence of (3.8b) and (4.1) using now in addition the bound on \ddot{x}_j^h . \square

Let us introduce the error $e_j(t) := x_j(t) - x_j^h(t)$. We infer from (3.11a) and (3.7a) that

(4.3)

$$\begin{aligned} \ddot{e}_j + \beta \dot{e}_j - \frac{2}{q_j^h + q_{j+1}^h} \frac{(\tau_{j+1} - \tau_{j+1}^h) - (\tau_j - \tau_j^h)}{h} \\ = (\dot{x}_j^h \cdot (\dot{\theta}_j^h - \tau_t(\rho_j, \cdot)) \tau(\rho_j, \cdot) + (\dot{x}_j^h \cdot \dot{\theta}_j^h) (\theta_j^h - \tau(\rho_j, \cdot)) - (\dot{e}_j \cdot \tau_t(\rho_j, \cdot)) \tau(\rho_j, \cdot) \\ + 2 \frac{(q_j^h - q_j) + (q_{j+1}^h - q_{j+1})}{(q_j + q_{j+1})(q_j^h + q_{j+1}^h)} \frac{\tau_{j+1} - \tau_j}{h} + R_j \\ =: \sum_{k=1}^5 T_j^k. \end{aligned}$$

Taking the scalar product with $\frac{h}{2}(q_j^h + q_{j+1}^h)\dot{e}_j$, summing over $j = 1, \dots, J$, and recalling Lemma 4.1 yields

$$\begin{aligned}
(4.4) \quad & \frac{1}{2}h \frac{d}{dt} \sum_{j=1}^J \frac{1}{2}(q_j^h + q_{j+1}^h)|\dot{e}_j|^2 + \beta h \sum_{j=1}^J \frac{1}{2}(q_j^h + q_{j+1}^h)|\dot{e}_j|^2 \\
& - h \sum_{j=1}^J \frac{(\tau_{j+1} - \tau_{j+1}^h) - (\tau_j - \tau_j^h)}{h} \cdot \dot{e}_j \\
& = \frac{1}{2}h \sum_{j=1}^J \frac{1}{2}(\dot{q}_j^h + \dot{q}_{j+1}^h)|\dot{e}_j|^2 + \sum_{k=1}^5 h \sum_{j=1}^J \frac{1}{2}(q_j^h + q_{j+1}^h)T_j^k \cdot \dot{e}_j \\
& \leq Ch \sum_{j=1}^J |\dot{e}_j|^2 + h \sum_{k=1}^5 \sum_{j=1}^J \frac{1}{2}(q_j^h + q_{j+1}^h)T_j^k \cdot \dot{e}_j.
\end{aligned}$$

While the above relation already provides us with some control on \dot{e}_j , the treatment of the elliptic part is more difficult. This is a consequence of the fact that the operator $\frac{1}{|x_\rho|} \left(\frac{x_\rho}{|x_\rho|} \right)_\rho$ is degenerate in the tangential direction. It is therefore not possible to directly control δe_j , which we split instead as follows:

$$(4.5) \quad \delta e_j = \delta x_j - \delta x_j^h = q_j(\tau_j - \tau_j^h) + (q_j - q_j^h)\tau_j^h.$$

In the next step, we will gain control on the difference of the tangents from the third term on the left-hand side of (4.4). To do so, we essentially adapt arguments from [4, section 5] developed for a finite element approach to the curve shortening flow. To begin, using summation by parts, together with the fact that $\delta x_j^h = q_j^h \tau_j^h$, we derive

$$\begin{aligned}
& -h \sum_{j=1}^J \frac{(\tau_{j+1} - \tau_{j+1}^h) - (\tau_j - \tau_j^h)}{h} \cdot \dot{e}_j \\
& = h \sum_{j=1}^J (\tau_j - \tau_j^h) \cdot \frac{\dot{e}_j - \dot{e}_{j-1}}{h} = h \sum_{j=1}^J (\tau_j - \tau_j^h) \cdot (\delta \dot{x}_j - \delta \dot{x}_j^h) \\
& = h \sum_{j=1}^J (\tau_j^h \cdot \delta \dot{x}_j^h - \tau_j \cdot \delta \dot{x}_j^h) + h \sum_{j=1}^J (\tau_j - \tau_j^h) \cdot \delta \dot{x}_j \\
& = h \frac{d}{dt} \sum_{j=1}^J (q_j^h - \tau_j \cdot \delta x_j^h) + h \sum_{j=1}^J \dot{\tau}_j \cdot \delta x_j^h + h \sum_{j=1}^J (\tau_j - \tau_j^h) \cdot \delta \dot{x}_j \\
& = h \frac{d}{dt} \sum_{j=1}^J q_j^h (1 - \tau_j \cdot \tau_j^h) + h \sum_{j=1}^J \frac{q_j^h}{q_j} (\delta \dot{x}_j - (\delta \dot{x}_j \cdot \tau_j) \tau_j) \cdot \tau_j^h + h \sum_{j=1}^J (\tau_j - \tau_j^h) \cdot \delta \dot{x}_j \\
& = \frac{1}{2}h \frac{d}{dt} \sum_{j=1}^J q_j^h |\tau_j - \tau_j^h|^2 + h \sum_{j=1}^J \left[\frac{q_j - q_j^h}{q_j} \delta \dot{x}_j \cdot (\tau_j - \tau_j^h) + \frac{1}{2} \frac{q_j^h}{q_j} (\delta \dot{x}_j \cdot \tau_j) |\tau_j - \tau_j^h|^2 \right].
\end{aligned}$$

If we insert the above relation into (4.4), note that $\beta \geq 0$, and apply a Cauchy–Schwarz inequality, together with Lemma 3.1 and (4.1), we obtain

$$\begin{aligned}
(4.6) \quad & \frac{1}{2}h \frac{d}{dt} \sum_{j=1}^J \left(\frac{1}{2}(q_j^h + q_{j+1}^h)|\dot{e}_j|^2 + q_j^h |\tau_j - \tau_j^h|^2 \right) \\
& \leq Ch \sum_{j=1}^J (|\dot{e}_j|^2 + (q_j - q_j^h)^2 + |\tau_j - \tau_j^h|^2) + h \sum_{k=1}^5 \sum_{j=1}^J \frac{1}{2}(q_j^h + q_{j+1}^h)T_j^k \cdot \dot{e}_j.
\end{aligned}$$

Let us next consider the terms involving $T_j^k, k = 1, \dots, 5$. To begin, note that (2.2) and (3.8a) imply

$$(4.7) \quad \tau(\rho_j, \cdot) \cdot \dot{e}_j = \tau(\rho_j, \cdot) \cdot (\dot{x}_j - \dot{x}_j^h) = -\tau(\rho_j, \cdot) \cdot \dot{x}_j^h = \dot{x}_j^h \cdot (\theta_j^h - \tau(\rho_j, \cdot)).$$

Therefore, the definition of T_j^1 in (4.3) yields that

$$\begin{aligned} & h \sum_{j=1}^J \frac{1}{2}(q_j^h + q_{j+1}^h) T_j^1 \cdot \dot{e}_j \\ &= h \sum_{j=1}^J \frac{1}{2}(q_j^h + q_{j+1}^h) (\dot{x}_j^h \cdot (\theta_j^h - \tau(\rho_j, \cdot))) (\dot{x}_j^h \cdot (\theta_j^h - \tau(\rho_j, \cdot))) \\ &= \frac{1}{2} h \frac{d}{dt} \sum_{j=1}^J \frac{1}{2}(q_j^h + q_{j+1}^h) (\dot{x}_j^h \cdot (\theta_j^h - \tau(\rho_j, \cdot)))^2 \\ &\quad - \frac{1}{2} h \sum_{j=1}^J \frac{1}{2}(q_j^h + q_{j+1}^h) (\dot{x}_j^h \cdot (\theta_j^h - \tau(\rho_j, \cdot)))^2 \\ &\quad - h \sum_{j=1}^J \frac{1}{2}(q_j^h + q_{j+1}^h) (\dot{x}_j^h \cdot (\theta_j^h - \tau(\rho_j, \cdot))) (\dot{x}_j^h \cdot (\theta_j^h - \tau(\rho_j, \cdot))) \\ &\leq \frac{1}{2} h \frac{d}{dt} \sum_{j=1}^J \frac{1}{2}(q_j^h + q_{j+1}^h) (\tau(\rho_j, \cdot) \cdot \dot{e}_j)^2 + Ch \sum_{j=1}^J |\theta_j^h - \tau(\rho_j, \cdot)|^2, \end{aligned}$$

where in the last step we have used (4.7), as well as Lemma 4.1. Moreover, we have from (3.6b) that

$$\begin{aligned} |\theta_j^h - \tau(\rho_j, \cdot)| &\leq \left| \frac{\tau_j^h + \tau_{j+1}^h}{|\tau_j^h + \tau_{j+1}^h|} - \frac{\tau_j + \tau_{j+1}}{|\tau_j + \tau_{j+1}|} \right| + \left| \frac{\tau_j + \tau_{j+1}}{|\tau_j + \tau_{j+1}|} - \tau(\rho_j, \cdot) \right| \\ &\leq \frac{2}{|\tau_j + \tau_{j+1}|} (|\tau_j - \tau_j^h| + |\tau_{j+1} - \tau_{j+1}^h|) + Ch^2, \end{aligned}$$

so that with (4.2a)

$$(4.8) \quad |\theta_j^h - \tau(\rho_j, \cdot)|^2 \leq C(|\tau_j - \tau_j^h|^2 + |\tau_{j+1} - \tau_{j+1}^h|^2) + Ch^4.$$

In particular, it follows that

$$(4.9) \quad h \sum_{j=1}^J \frac{1}{2}(q_j^h + q_{j+1}^h) T_j^1 \cdot \dot{e}_j \leq \frac{1}{2} h \frac{d}{dt} \sum_{j=1}^J \frac{1}{2}(q_j^h + q_{j+1}^h) (\tau(\rho_j, \cdot) \cdot \dot{e}_j)^2 + Ch \sum_{j=1}^J |\tau_j - \tau_j^h|^2 + Ch^4.$$

Next, we deduce with the help of Lemma 4.1, (4.1), and (4.8) that

$$(4.10) \quad h \sum_{j=1}^J \frac{1}{2}(q_j^h + q_{j+1}^h) T_j^2 \cdot \dot{e}_j \leq Ch \sum_{j=1}^J |\theta_j^h - \tau(\rho_j, \cdot)| |\dot{e}_j| \leq Ch \sum_{j=1}^J (|\tau_j - \tau_j^h|^2 + |\dot{e}_j|^2) + Ch^4,$$

while in view of (3.12),

$$(4.11) \quad h \sum_{j=1}^J \frac{1}{2} (q_j^h + q_{j+1}^h) (T_j^3 + T_j^5) \cdot \dot{e}_j \leq Ch \sum_{j=1}^J |\dot{e}_j|^2 + Ch^4.$$

Finally, with the help of (3.6c) and (2.6) we can bound

$$(4.12) \quad h \sum_{j=1}^J \frac{1}{2} (q_j^h + q_{j+1}^h) T_j^4 \cdot \dot{e}_j \leq Ch \sum_{j=1}^J (|q_j - q_j^h| + |q_{j+1} - q_{j+1}^h|) \frac{|\tau_{j+1} - \tau_j|}{h} |\dot{e}_j| \\ \leq Ch \sum_{j=1}^J ((q_j - q_j^h)^2 + |\dot{e}_j|^2) + Ch^4.$$

If we insert (4.9), (4.10), (4.11), and (4.12) into the estimate (4.6), we obtain, upon subtracting the first term on the right-hand side of (4.9) from both sides of the inequality and on noting $|\dot{e}_j|^2 - (\dot{e}_j \cdot \tau)^2 = (\dot{e}_j \cdot \nu)^2$, that

$$(4.13) \quad \frac{1}{2} h \frac{d}{dt} \sum_{j=1}^J \left(\frac{1}{2} (q_j^h + q_{j+1}^h) (\dot{e}_j \cdot \nu(\rho_j, \cdot))^2 + q_j^h |\tau_j - \tau_j^h|^2 \right) \\ \leq Ch \sum_{j=1}^J (|\dot{e}_j|^2 + (q_j - q_j^h)^2 + |\tau_j - \tau_j^h|^2) + Ch^4.$$

Using (4.7), (4.8), and Lemma 4.1, we have

$$(4.14) \quad h \sum_{j=1}^J |\dot{e}_j|^2 = h \sum_{j=1}^J ((\dot{e}_j \cdot \tau(\rho_j, \cdot))^2 + (\dot{e}_j \cdot \nu(\rho_j, \cdot))^2) \\ = h \sum_{j=1}^J (\dot{x}_j^h \cdot (\theta_j^h - \tau(\rho_j, \cdot)))^2 + h \sum_{j=1}^J (\dot{e}_j \cdot \nu(\rho_j, \cdot))^2 \\ \leq Ch \sum_{j=1}^J |\tau_j - \tau_j^h|^2 + Ch^4 + h \sum_{j=1}^J (\dot{e}_j \cdot \nu(\rho_j, \cdot))^2.$$

If we insert (4.14) into (4.13), we find

$$(4.15) \quad \phi_h'(t) \leq C_3 (h^4 + \phi_h(t) + \psi_h(t)),$$

where we have abbreviated

$$(4.16) \quad \phi_h(t) := h \sum_{j=1}^J \left(\frac{1}{2} (q_j^h + q_{j+1}^h) (\dot{e}_j \cdot \nu(\rho_j, \cdot))^2 + q_j^h |\tau_j - \tau_j^h|^2 \right), \quad \psi_h(t) := h \sum_{j=1}^J (q_j - q_j^h)^2$$

and noted (4.1).

It remains to bound the function ψ_h , which controls the second part in (4.5). To do so, we combine (3.11b) and (3.8b) and obtain

(4.17)

$$\begin{aligned} \dot{q}_j - \dot{q}_j^h &= -\frac{1}{4}(q_{j-1} + q_j)(\dot{x}_{j-1} \cdot \ddot{x}_{j-1} - \dot{x}_{j-1}^h \cdot \ddot{x}_{j-1}^h) - \frac{1}{4}(q_j + q_{j+1})(\dot{x}_j \cdot \ddot{x}_j - \dot{x}_j^h \cdot \ddot{x}_j^h) \\ &\quad + \frac{1}{4}((q_{j-1}^h - q_{j-1}) + (q_j^h - q_j))\dot{x}_{j-1}^h \cdot \ddot{x}_{j-1}^h + \frac{1}{4}((q_j^h - q_j) + (q_{j+1}^h - q_{j+1}))\dot{x}_j^h \cdot \ddot{x}_j^h \\ &\quad - \frac{1}{4}\beta(q_{j-1} + q_j)(|\dot{x}_{j-1}|^2 - |\dot{x}_{j-1}^h|^2) - \frac{1}{4}\beta(q_j + q_{j+1})(|\dot{x}_j|^2 - |\dot{x}_j^h|^2) \\ &\quad + \frac{1}{4}\beta((q_{j-1}^h - q_{j-1}) + (q_j^h - q_j))|\dot{x}_{j-1}^h|^2 + \frac{1}{4}\beta((q_j^h - q_j) + (q_{j+1}^h - q_{j+1}))|\dot{x}_j^h|^2 + \tilde{R}_j \\ &= -\frac{1}{8}\partial_t((q_{j-1} + q_j)(|\dot{x}_{j-1}|^2 - |\dot{x}_{j-1}^h|^2)) - \frac{1}{8}\partial_t((q_j + q_{j+1})(|\dot{x}_j|^2 - |\dot{x}_j^h|^2)) \\ &\quad + \frac{1}{8}(\dot{q}_{j-1} + \dot{q}_j)(|\dot{x}_{j-1}|^2 - |\dot{x}_{j-1}^h|^2) + \frac{1}{8}(\dot{q}_j + \dot{q}_{j+1})(|\dot{x}_j|^2 - |\dot{x}_j^h|^2) \\ &\quad + \frac{1}{4}((q_{j-1}^h - q_{j-1}) + (q_j^h - q_j))\dot{x}_{j-1}^h \cdot \ddot{x}_{j-1}^h + \frac{1}{4}((q_j^h - q_j) + (q_{j+1}^h - q_{j+1}))\dot{x}_j^h \cdot \ddot{x}_j^h \\ &\quad - \frac{1}{4}\beta(q_{j-1} + q_j)(|\dot{x}_{j-1}|^2 - |\dot{x}_{j-1}^h|^2) - \frac{1}{4}\beta(q_j + q_{j+1})(|\dot{x}_j|^2 - |\dot{x}_j^h|^2) \\ &\quad + \frac{1}{4}\beta((q_{j-1}^h - q_{j-1}) + (q_j^h - q_j))|\dot{x}_{j-1}^h|^2 + \frac{1}{4}\beta((q_j^h - q_j) + (q_{j+1}^h - q_{j+1}))|\dot{x}_j^h|^2 + \tilde{R}_j. \end{aligned}$$

Recalling (1.4b) and (3.7b), we infer that $q_j^h(0) = q_j(0)$ as well as

$$(4.18) \quad |\dot{e}_j(0)| = |\dot{x}_j(0) - \dot{x}_j^h(0)| = \left| \mathcal{V}_0(\rho_j) \left(\tau(\rho_j, 0) - \frac{\tau_j(0) + \tau_{j+1}(0)}{|\tau_j(0) + \tau_{j+1}(0)|} \right)^\perp \right| \leq Ch^2,$$

where we also made use of (3.6b). Thus, we obtain after integrating (4.17) in time, on noting that $||a|^2 - |b|^2| \leq (|a| + |b|)|a - b|$ and on taking into account Lemma 4.1 and (3.12), that

$$\begin{aligned} |q_j(t) - q_j^h(t)| &\leq C(|\dot{e}_{j-1}(t)| + |\dot{e}_j(t)|) + C \int_0^t |\dot{e}_{j-1}(u)| + |\dot{e}_j(u)| \, du \\ &\quad + C \int_0^t |(q_{j-1} - q_{j-1}^h)(u)| + |(q_j - q_j^h)(u)| + |(q_{j+1} - q_{j+1}^h)(u)| \, du + Ch^2 \\ &\leq C(|\dot{e}_{j-1}(t)| + |\dot{e}_j(t)|) + C \left(\int_0^t |\dot{e}_{j-1}(u)|^2 + |\dot{e}_j(u)|^2 \, du \right)^{\frac{1}{2}} \\ &\quad + C \left(\int_0^t |(q_{j-1} - q_{j-1}^h)(u)|^2 + |(q_j - q_j^h)(u)|^2 + |(q_{j+1} - q_{j+1}^h)(u)|^2 \, du \right)^{\frac{1}{2}} + Ch^2. \end{aligned}$$

Taking the square and summing over j yields

$$\begin{aligned} h \sum_{j=1}^J (q_j - q_j^h)^2(t) &\leq Ch \sum_{j=1}^J |\dot{e}_j(t)|^2 + C \int_0^t h \sum_{j=1}^J |\dot{e}_j(u)|^2 \, du + Ch \int_0^t (q_j - q_j^h)^2(u) \, du + Ch^4, \end{aligned}$$

which together with (4.14) and (4.1) implies

$$(4.19) \quad \psi_h(t) \leq C_4 \left(\phi_h(t) + \int_0^t (\phi_h(u) + \psi_h(u)) \, du + h^4 \right).$$

If we multiply (4.15) by $2C_4$, integrate with respect to time, and combine the result with (4.19), we obtain, on noting from (4.18) that $\phi_h(0) \leq C_5h^4$, that

$$C_4\phi_h(t) + \psi_h(t) \leq (2C_4(C_3 + C_5) + C_4) \left(h^4 + \int_0^t \phi_h(u) + \psi_h(u) \, du \right),$$

from which we deduce with the help of Gronwall’s lemma that

$$(4.20) \quad \phi_h(t) + \psi_h(t) \leq Ch^4, \quad 0 \leq t < \widehat{T}_h.$$

In particular, we have for $j = 1, \dots, J$ and $0 \leq t < \widehat{T}_h$ that

$$(4.21) \quad |(\tau_j - \tau_j^h)(t)| \leq h^{-\frac{1}{2}} \left(h \sum_{k=1}^J |(\tau_k - \tau_k^h)(t)| \right)^{\frac{1}{2}} \leq Ch^{-\frac{1}{2}} \sqrt{\phi_h(t)} \leq Ch^{\frac{3}{2}} \leq \frac{1}{2}h^{\frac{5}{4}},$$

provided that $0 < h \leq h_0$ and h_0 is chosen smaller if necessary. In a similar way, on combining (4.20), (4.16), (4.14), (3.5), and (2.6), we obtain that

$$|(\dot{x}_j - \dot{x}_j^h)(t)| \leq \frac{1}{2}h^{\frac{5}{4}}, \quad \frac{1}{3}c_0 \leq q_j^h(t) \leq 3C_0, \quad j = 1, \dots, J, \quad 0 \leq t < \widehat{T}_h.$$

If $\widehat{T}_h < T$, one could therefore continue the discrete solution to an interval $[0, \widehat{T}_h + \varepsilon]$, for some $\varepsilon > 0$, such that $\frac{1}{4}c_0 \leq q_j^h(t) \leq 4C_0$, $|\tau_j(t) - \tau_j^h(t)| + |\dot{x}_j(t) - \dot{x}_j^h(t)| \leq h^{\frac{5}{4}}$ for all $j = 1, \dots, J$, and $0 \leq t \leq \widehat{T}_h + \varepsilon$, contradicting the definition of \widehat{T}_h . Thus, $\widehat{T}_h = T$. Finally, the bounds (3.13) follow from (4.20), the definitions of ϕ_h and ψ_h , (4.14), and (4.5).

5. Numerical results.

5.1. Fully discrete scheme. For the numerical simulations presented in this section, we consider the following fully discrete approximation of (3.7), where in order to discretize in time, we let $t_m = m\Delta t$, $m = 0, \dots, M$, with the uniform time step $\Delta t = \frac{T}{M} > 0$. We will approximate $x^h(t_m)$ by the grid function $x^m : \mathcal{G}^h \rightarrow \mathbb{R}^2$. Analogously to (3.3), we define θ_j^m , $j = 1, \dots, J$, in terms of x^m , and similarly for q_j^m and τ_j^m . Then, given suitable initial data $x^0, x^{-1} : \mathcal{G}^h \rightarrow \mathbb{R}^2$, for $m = 0, \dots, M - 1$ we find $x^{m+1} : \mathcal{G}^h \rightarrow \mathbb{R}^2$ such that, for $j = 1, \dots, J$,

$$(5.1) \quad \begin{aligned} & \frac{1}{2}(q_j^m + q_{j+1}^m)h \frac{x_j^{m+1} - 2x_j^m + x_j^{m-1}}{(\Delta t)^2} + \frac{1}{4}\beta(q_j^m + q_{j+1}^m)h \frac{x_j^{m+1} - x_j^{m-1}}{\Delta t} \\ &= \frac{1}{2q_{j+1}^m} \delta x_{j+1}^{m+1} - \frac{1}{2q_j^m} \delta x_j^{m+1} + \frac{1}{2q_{j+1}^m} \delta x_{j+1}^{m-1} - \frac{1}{2q_j^m} \delta x_j^{m-1} \\ & \quad - \frac{1}{2}(q_j^m + q_{j+1}^m)h \left(\frac{x_j^m - x_j^{m-1}}{\Delta t} \cdot \frac{\theta_j^m - \theta_j^{m-1}}{\Delta t} \right) \theta_j^m. \end{aligned}$$

Observe that we have chosen a linear discretization that is analogous to a mass-lumped finite element approximation of (1.4a), which uses a semi-implicit approximation of $\frac{1}{|x_\rho|} \left(\frac{x_\rho}{|x_\rho|} \right)_\rho$ in the spirit of the discretizations proposed for the linear wave equation in, e.g., [10, section 2.7]. We remark that in contrast to the semidiscrete setting (recall (3.8a)), it does not appear possible to prove a fully discrete analogue of the crucial normal flow property (2.2) for the fully discrete scheme (5.1).

In order to derive suitable initial data for (5.1), we observe that the solution to (1.4) satisfies the Taylor expansion

$$(5.2) \quad \begin{aligned} x(\cdot, \Delta t) &= x + \Delta t x_t + \frac{1}{2}(\Delta t)^2 x_{tt} + \mathcal{O}((\Delta t)^3) \\ &= x + \Delta t \mathcal{V}_0 \nu + \frac{1}{2}(\Delta t)^2 \left[\frac{1}{|x_\rho|} \left(\frac{x_\rho}{|x_\rho|} \right)_\rho - (\mathcal{V}_0 \nu \cdot \tau_t) \tau - \beta \mathcal{V}_0 \nu \right] + \mathcal{O}((\Delta t)^3) \\ &= x + \Delta t \mathcal{V}_0 \nu + \frac{1}{2}(\Delta t)^2 \left[\frac{1}{|x_\rho|} \left(\frac{x_\rho}{|x_\rho|} \right)_\rho - \frac{1}{|x_\rho|} \mathcal{V}_0 \mathcal{V}_{0,\rho} \tau - \beta \mathcal{V}_0 \nu \right] + \mathcal{O}((\Delta t)^3), \end{aligned}$$

where on the right-hand side we always evaluate $x, \tau, \nu, \mathcal{V}_0$ and their derivatives at $(\cdot, 0)$. Note in particular that in the last step we used that

$$\tau_t \cdot \nu = \frac{x_{t,\rho}}{|x_\rho|} \cdot \nu = \frac{1}{|x_\rho|} (\mathcal{V}_0 \nu)_\rho \cdot \nu = \frac{1}{|x_\rho|} \mathcal{V}_{0,\rho}$$

Inspired by (5.2), we choose as initial data

$$\begin{aligned} x_j^0 &= x_0(\rho_j) \quad \text{and} \\ x_j^{-1} &= x_j^0 - \Delta t \mathcal{V}_0(\rho_j) \theta_j^{0,\perp} \\ &\quad + \frac{1}{2} (\Delta t)^2 \left[\frac{2}{q_j^0 + q_{j+1}^0} \left(\frac{1}{h} \left(\frac{\delta x_{j+1}^0}{q_{j+1}^0} - \frac{\delta x_j^0}{q_j^0} \right) - \mathcal{V}_0(\rho_j) \mathcal{V}_{0,\rho}(\rho_j) \theta_j^{0,\perp} \right) - \beta V_0 \theta_j^{0,\perp} \right] \end{aligned}$$

for $j = 1, \dots, J$.

We stress that all our presented numerical experiments fall within the scope of our main result, Theorem 3.5. However, for nonconvex initial data, and for convex initial data with an initial normal velocity \mathcal{V}_0 such that $\max_I \mathcal{V}_0 > 0$, a rigorous existence and regularity theory for the underlying PDE appears to be still lacking.

5.2. Convergence experiment. Our first set of numerical experiments is for the evolution of an initially circular curve when $\beta = 0$. It can be shown that a family of circles with radius $r(t)$ is a solution to (1.2) with $\mathcal{V}_\Gamma|_{t=0} = V_0 \in \mathbb{R}$ for the initial outer normal velocity if

$$\ddot{r}(t) = -\frac{1}{r(t)} \quad \text{in } (0, T], \quad r(0) = r_0, \quad \dot{r}(0) = V_0.$$

Upon integration we obtain that

$$\frac{1}{2} (\dot{r}(t))^2 = \ln r_0 - \ln r(t) + \frac{1}{2} V_0^2 = \ln \frac{r_0}{r(t)} + \frac{1}{2} V_0^2.$$

Hence,

$$\dot{r}(t) = \pm \sqrt{2 \ln \frac{r_0}{r(t)} + V_0^2},$$

which means that if $V_0 > 0$, then $r(t)$ will at first increase until it hits a maximum, where $2 \ln \frac{r_0}{r(t)} + V_0^2 = 0$, after which it will decrease and shrink to a point in finite time. On the other hand, if $V_0 \leq 0$, then the circle will monotonically shrink to a point.

For the special case $V_0 = 0$, and on recalling the Gauss error function

$$\operatorname{erf}(z) = \frac{2}{\sqrt{\pi}} \int_0^z e^{-u^2} du, \quad \operatorname{erf}'(z) = \frac{2}{\sqrt{\pi}} e^{-z^2},$$

we find that $r(t)$ is the solution of

$$t - \sqrt{\frac{\pi}{2}} r_0 \operatorname{erf} \left(\sqrt{\ln \frac{r_0}{r(t)}} \right) = 0,$$

which means that

$$(5.3) \quad r(t) = r_0 \exp \left(- \left[\operatorname{erf}^{-1} \left(\sqrt{\frac{2}{\pi}} \frac{t}{r_0} \right) \right]^2 \right).$$

TABLE 1

Errors for the convergence test for (5.4), (5.3) with $r_0 = 1$ over the time interval $[0, 1]$ for the scheme (5.1). We also display the experimental orders of convergence (EOC).

J	$\max_{m=0, \dots, M} \ x(t_m) - x^m\ _{1,h}$	EOC	$\max_{m=1, \dots, M-1} \ \dot{x}(t_m) - \frac{x^{m+1} - x^{m-1}}{2\Delta t}\ _{0,h}$	EOC
32	3.9796e-03	—	9.5331e-04	—
64	1.0059e-03	1.98	2.4960e-04	1.93
128	2.5256e-04	1.99	6.3995e-05	1.96
256	6.3254e-05	2.00	1.6211e-05	1.98
512	1.5827e-05	2.00	4.0803e-06	1.99
1024	3.9582e-06	2.00	1.0236e-06	2.00
2048	9.8980e-07	2.00	2.5634e-07	2.00

For the true solution

$$(5.4) \quad x(\rho, t) = r(t) \begin{pmatrix} \cos g(2\pi\rho) \\ \sin g(2\pi\rho) \end{pmatrix}, \quad g(u) = u + 0.1 \sin(u)$$

of (1.4), we compute approximations to the errors between x and x^h , the solution to (3.7) with $\mathcal{V}_0 = 0$, for the choice $r_0 = 1$ on the time interval $[0, 1]$ with the help of the fully discrete scheme (5.1). In particular, for the sequence of discretization parameters $h = \frac{1}{j} = 2^{-k}$, $k = 5, \dots, 11$, we let $\Delta t = h$ and compare the grid interpolations of x and \dot{x} to their fully discrete analogues in the discrete norms (3.2). These errors are reported in Table 1, where we observe the expected second order convergence rates from Theorem 3.5.

5.3. Numerical experiments with constant initial velocity. Throughout the remainder of the numerical results section we choose the discretization parameters $J = 256$ and $\Delta t = 10^{-4}$. Moreover, we always let $\beta = 0$, unless stated otherwise. The curve evolutions we visualize by plotting the polygonal curves $\Gamma^m \subset \mathbb{R}^2$ defined by the vertices $\{x_j^m\}_{j=1}^J$, and at times we also show the evolution of the length of these curves, defined by

$$|\Gamma^m| = h \sum_{j=1}^J q_j^m = \sum_{j=1}^J |x_j^m - x_{j-1}^m|.$$

Moreover, we will often be interested in a possible blow-up in curvature, and so we will monitor the quantity

$$K_\infty^m = \max_{j=1, \dots, J} \frac{|\delta\tau_j^m|}{q_j^m}$$

as an approximation to the maximal value of $|\varkappa| = \frac{|\tau_\rho|}{|x_\rho|}$; recall (1.3).

In all the numerical computations in this subsection, we will choose a constant initial velocity $\mathcal{V}_0(\rho) = V_0$.

As discussed above, for an initial circle with uniform initial normal velocity $\mathcal{V}_0 = V_0$, depending on the sign of $V_0 \in \mathbb{R}$ the family of circles either expands at first and then shrinks, or it shrinks immediately. We visualize these different behaviors in Figure 1. In each case, we observe a smooth solution until the circles shrink to a point, meaning that $|\Gamma^m|$ and $1/K_\infty^m$ approach zero at the same time.

For the next computations, we choose as initial curve a mild ellipse, with a major axis of length 3 and a minor axis of length 2. The results for $V_0 = 0$ are shown

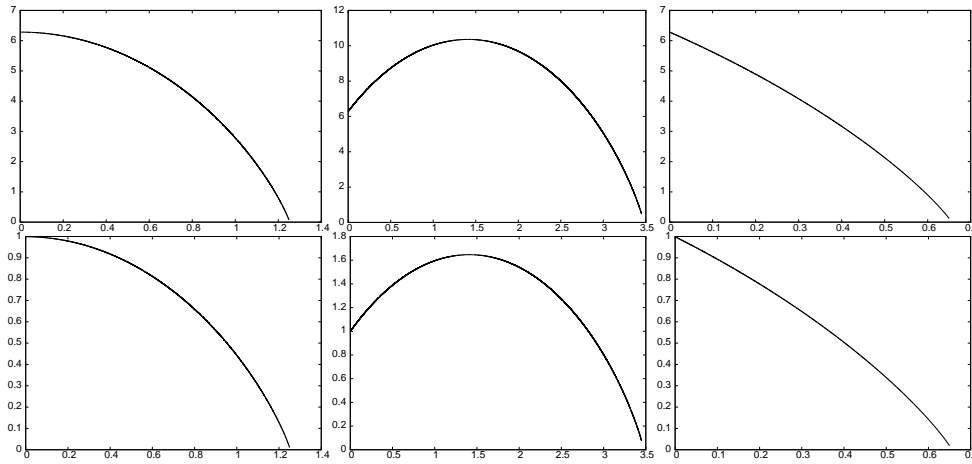


FIG. 1. Hyperbolic curvature flow starting from a unit circle. Above we show the evolution of $|\Gamma^m|$ over time for $V_0 = 0$, $V_0 = 1$, and $V_0 = -1$ (from left to right). The final times for these computations are $T = 1.25$, $T = 3.45$, and $T = 0.65$, respectively. Below we show the corresponding evolutions of $1/K_\infty^m$ over time.

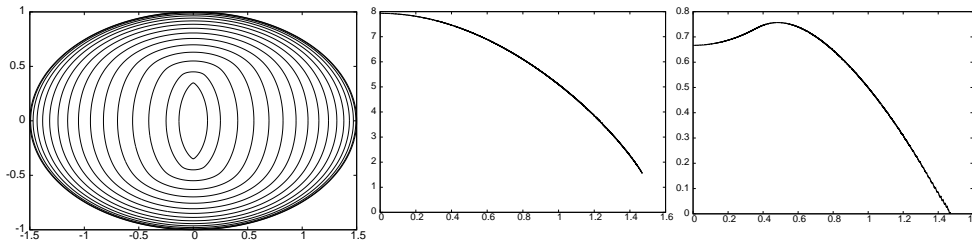


FIG. 2. Hyperbolic curvature flow, with $V_0 = 0$, starting from an ellipse. On the left we show Γ^m at times $t = 0, 0.1, \dots, 1.4, T = 1.47$. We also show the evolutions of $|\Gamma^m|$ (middle) and $1/K_\infty^m$ (right) over time.

in Figure 2, where we note the onset of a singularity in finite time. In particular, the curve appears to form two kinks, leading to a blow-up in curvature. When we choose the initial normal velocity as $V_0 = 1$, we obtain the results shown in Figure 3. Once again we observe a blow-up in curvature, although this time the curve does not exhibit two kinks. Instead it seems to approach a shape with four corners. We note that the initial ellipse at first grows towards a circle. It then shrinks while momentarily adopting an elliptic shape but with the major and minor axes swapped with respect to the initial data. Towards the end of the evolution a more circular shape appears again, which then evolves to the limiting shape with the four corners, i.e., with four points where the curvature is discontinuous. We stress that the observed singularities in our numerical simulations are robust with respect to the choice of discretization parameters. For example, refining the discretization parameters to $J = 512$ and $\Delta t = 5 \times 10^{-5}$ gave visually indistinguishable results compared to Figure 3.

We are interested in the effect of the parameter β on these developing singularities and would expect some damping or smoothing to be observable for $\beta > 0$. Repeating the simulation from Figure 2 with $\beta = 2$ yields the results in Figure 4, where we observe that the blow-up in curvature now happens much later, when the curve itself

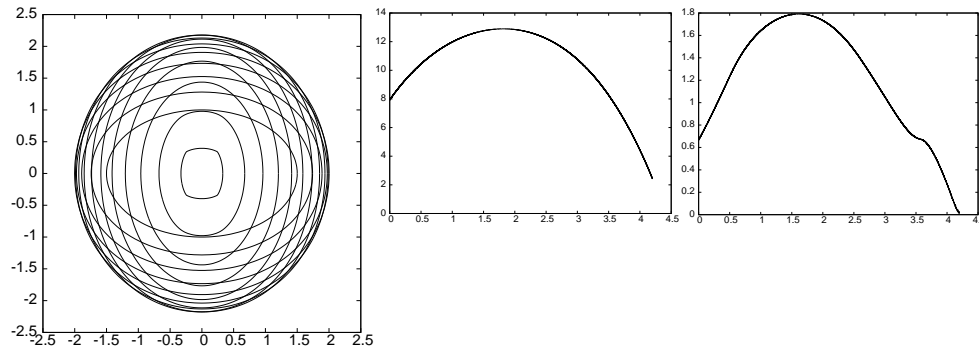


FIG. 3. Hyperbolic curvature flow, with $V_0 = 1$, starting from an ellipse. On the left we show Γ^m at times $t = 0, 0.3, \dots, T = 4.2$. We also show the evolutions of $|\Gamma^m|$ (middle) and $1/K_\infty^m$ (right) over time.

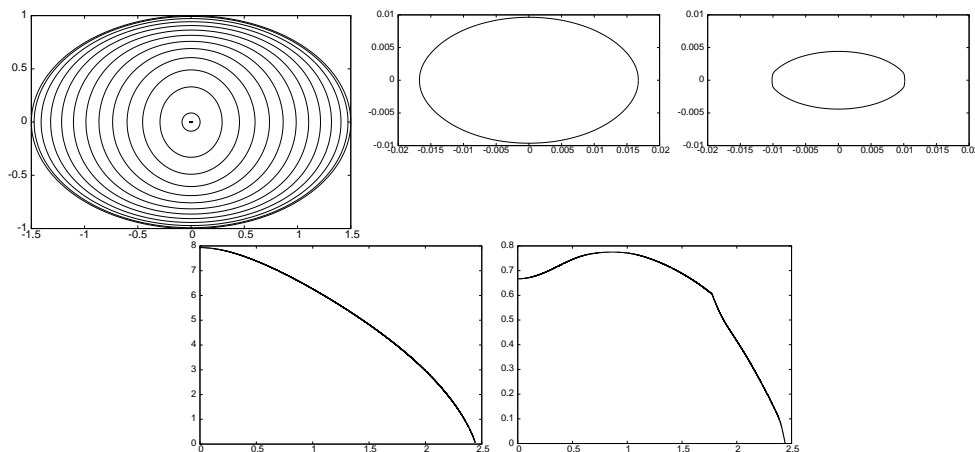


FIG. 4. Damped hyperbolic curvature flow, with $\beta = 2$ and $V_0 = 0$, starting from an ellipse. On the top we show Γ^m at times $t = 0, 0.2, \dots, 2.4, T = 2.4423$, as well as Γ^m separately at times $t = 2.44$ and $t = T$. Below we show the evolutions of $|\Gamma^m|$ (left) and $1/K_\infty^m$ (right) over time.

is almost extinct. We also see a marked change in the profile of the evolving curve. While in Figure 2 at late times the curve resembles an ellipsoid aligned with the x_2 -axis, the evolution in Figure 4 for long times appears to approach a circle, until towards the very end it starts to resemble an ellipsoid aligned with the x_1 -axis. In addition, a repeat of Figure 3 now with $\beta = 0.1$ is shown in Figure 5, where once again we note that visually the curve appears smoother for longer, until eventually the curvature blows up due to faceting on the left and right sides of the curve.

Finally, we also consider some numerical experiments where the initial data is nonconvex. For the simulation in Figure 6, we start from a smooth dumbbell-like initial curve. We observe that the curve starts to shrink until it eventually exhibits two facets on the left and right, which leads to a blow-up in the curvature. Repeating the simulation for the constant initial velocity $V_0 = 1$ yields the results in Figure 7. Now the curve first expands vertically into a convex curve that expands further, until it narrows on the x_1 -axis towards the origin to create a new nonconvex shape that resembles a variant of the initial data that is now aligned with the x_2 -axis.

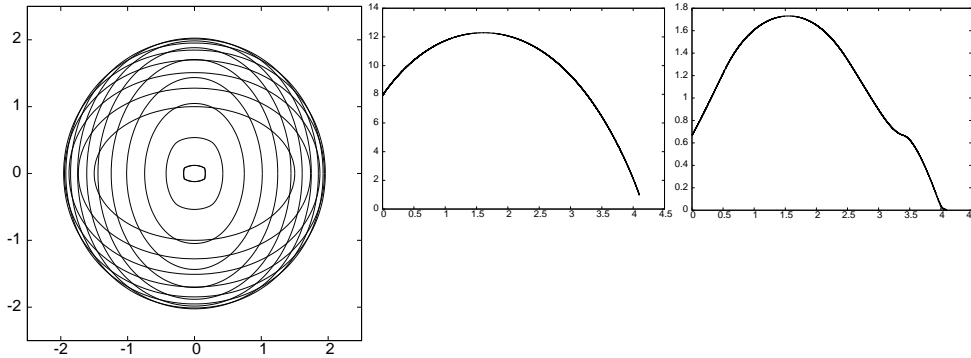


FIG. 5. Damped hyperbolic curvature flow, with $\beta = 0.1$ and $V_0 = 1$, starting from an ellipse. On the left we show Γ^m at times $t = 0, 0.3, \dots, 3.9, T = 4.1$. We also show the evolutions of $|\Gamma^m|$ (middle) and $1/K_\infty^m$ (right) over time.

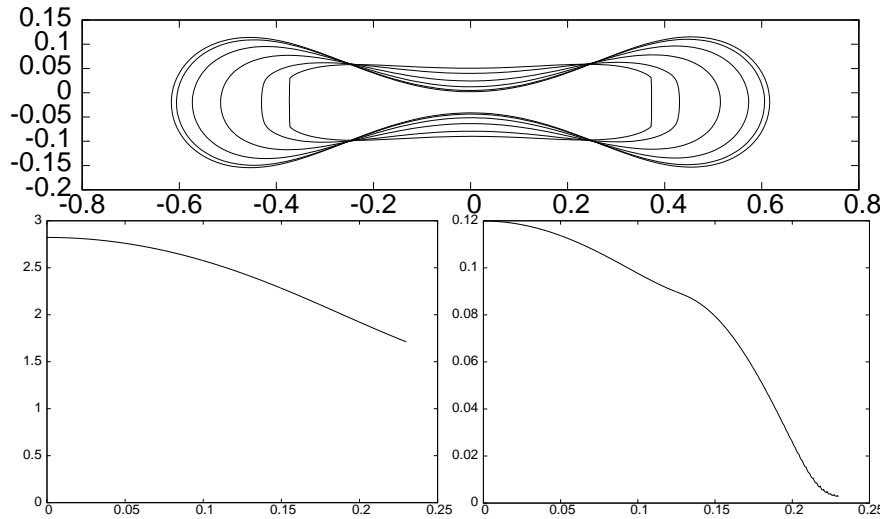


FIG. 6. Hyperbolic curvature flow, with $V_0 = 0$, starting from a smooth dumbbell. On top we show Γ^m at times $t = 0, 0.05, \dots, 0.2, T = 0.23$. Below we show the evolutions of $|\Gamma^m|$ (left) and $1/K_\infty^m$ (right) over time.

At this stage the curve begins again to expand into a convex shape that then shrinks until two developing kinks at the top and bottom of the curve lead to a blow-up in curvature. Interestingly, when we use the initial velocity $V_0 = -1$ the curve soon self-intersects (see Figure 8), which is something the parametric formulation is blind towards. Similarly to the evolution in Figure 6, the solution approaches a blow-up in curvature when two facets are about to be created on the left and right sides of the curve.

In conclusion, we remark that the onset of a blow-up in curvature in finite time for strictly convex initial data as observed in Figure 2 confirms the theoretical predictions in [15]. In addition, Figure 3 demonstrates that the same can be observed for an outward initial velocity $V_0\nu(\cdot, 0)$. Finally, from our remaining numerical simulations we conjecture that also nonconvex initial data can exhibit the same phenomenon.

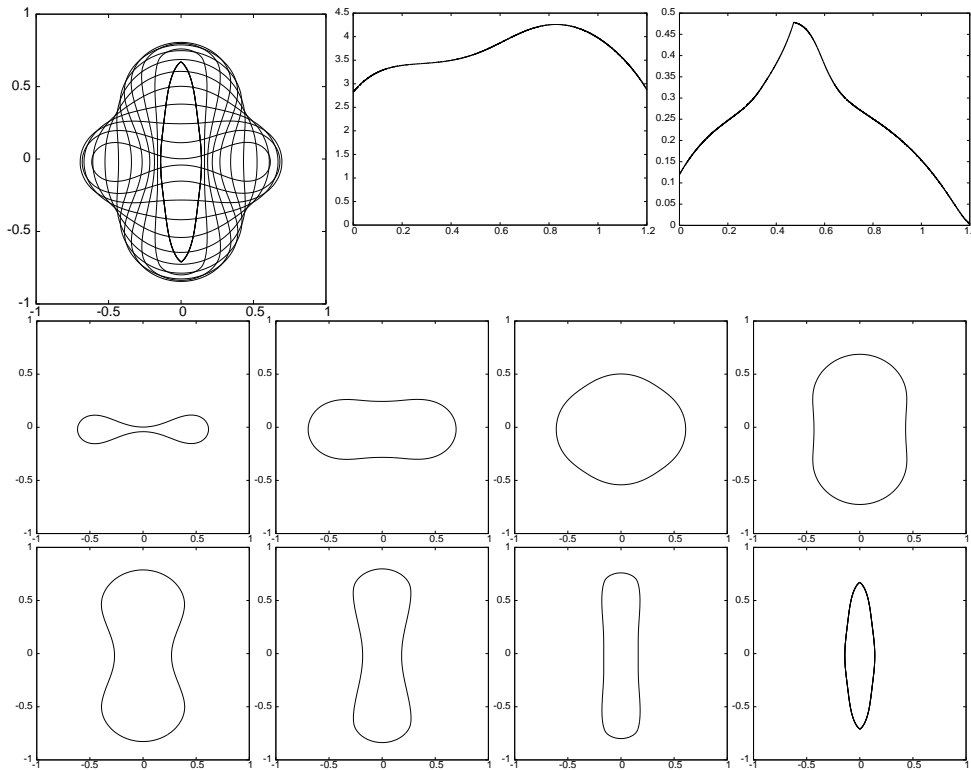


FIG. 7. Hyperbolic curvature flow, with $V_0 = 1$, starting from a smooth dumbbell. On top we show Γ^m at times $t = 0, 0.1, \dots, T = 1.2$ (left), as well as evolutions of $|\Gamma^m|$ (middle) and $1/K_\infty^m$ (right) over time. Below we visualize Γ^m separately at times $t = 0, 0.2, 0.4, 0.6$ and $0.8, 1, 1.1, 1.2$.

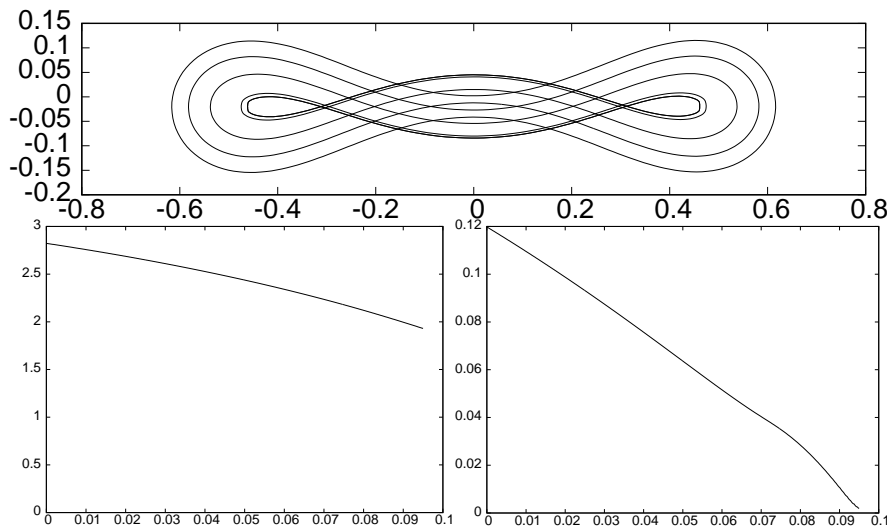


FIG. 8. Hyperbolic curvature flow, with $V_0 = -1$, starting from a smooth dumbbell. On top we show Γ^m at times $t = 0, 0.03, \dots, 0.09, T = 0.095$. Below we show the evolutions of $|\Gamma^m|$ (left) and $1/K_\infty^m$ (right) over time.

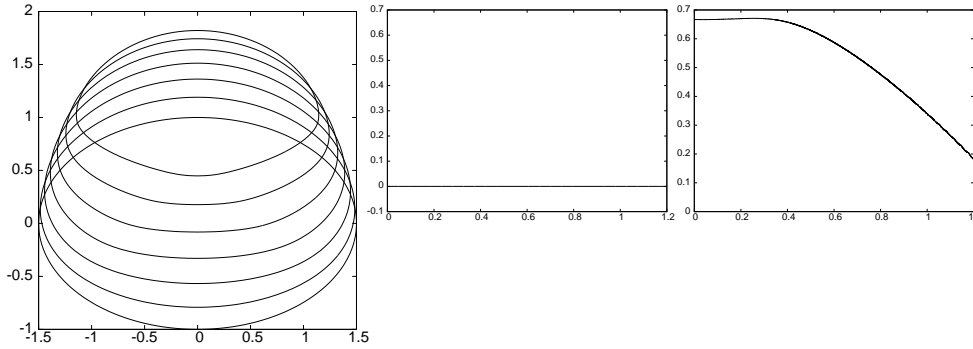


FIG. 9. Hyperbolic curvature flow, with $\mathcal{V}_0(\rho) = \sin(2\pi\rho)$, starting from an ellipse parameterized by $x_0(\rho) = (\frac{3}{2} \cos(2\pi\rho), \sin(2\pi\rho))^T$. On the left we show Γ^m at times $t = 0, 0.2, \dots, T = 1.2$. We also show the evolutions of $\|D_t x^{m+1} \cdot \theta^m\|_{0,h}$ (middle) and $1/K_\infty^m$ (right) over time.

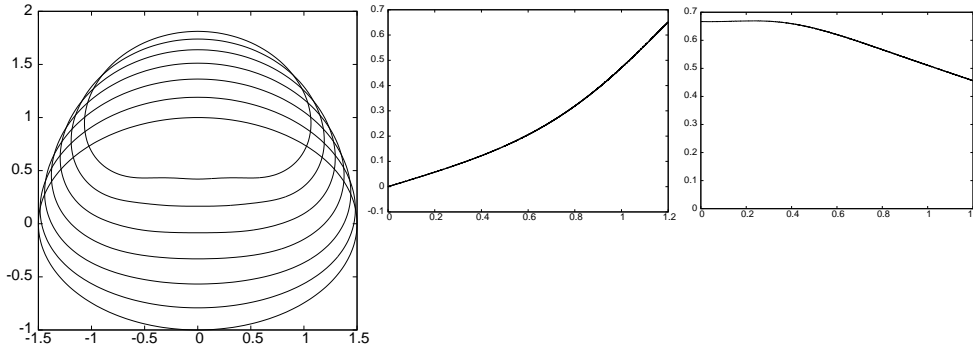


FIG. 10. The flow (1.5) with (1.4b) for $\mathcal{V}_0(\rho) = \sin(2\pi\rho)$, starting from an ellipse parameterized by $x_0(\rho) = (\frac{3}{2} \cos(2\pi\rho), \sin(2\pi\rho))^T$. On the left we show Γ^m at times $t = 0, 0.2, \dots, T = 1.2$. We also show the evolutions of $\|D_t x^{m+1} \cdot \theta^m\|_{0,h}$ (middle) and $1/K_\infty^m$ (right) over time.

5.4. Numerical experiments with nonconstant initial velocity. In this final subsection, we report on a numerical simulation with a nonconstant initial velocity \mathcal{V}_0 . In particular, we repeat the experiment from Figure 3, but now choose $\mathcal{V}_0(\rho) = \sin(2\pi\rho)$, with $x_0(\rho) = (\frac{3}{2} \cos(2\pi\rho), \sin(2\pi\rho))^T$. The evolution can be seen in Figure 9. Note that due to the given initial velocity, the curve rises and shrinks at the same time. Towards the end of the evolution a flat patch appears to develop at the bottom part of the curve. For a later comparison, we also provide a plot of the discrete tangential velocity

$$\|D_t x^{m+1} \cdot \theta^m\|_{0,h} := \left(h \sum_{j=1}^J \left| \frac{x_j^{m+1} - x_j^m}{\Delta t} \cdot \theta_j^m \right|^2 \right)^{\frac{1}{2}}$$

over time in Figure 9. Since (5.1) is a discrete approximation of the normal flow (1.4), the quantity stays nearly equal to zero throughout the evolution.

We mentioned in the introduction that a question of mathematical interest is whether solutions to (1.5) parameterize curves evolving according to (1.2). We now

Downloaded 07/25/23 to 193.205.210.74 . Redistribution subject to SIAM license or copyright; see https://pubs.siam.org/terms-privacy

provide some numerical evidence that this is not the case. In order to numerically approximate solutions to (1.5), we naturally adapt the scheme (5.1), for $\beta = 0$, by omitting the last term on the right-hand side of (5.1). For this new scheme, we then repeat the computation from Figure 9 using exactly the same discrete initial data. The ensuing evolution, shown in Figure 10, is close to what we observed before but ultimately differs. The differences are most pronounced in the final shape of Γ^m and in the plot of $1/K_\infty^m$ over time. We remark that a main difference between (1.4) and (1.5) is that the former is a normal flow, while the latter allows for a nonzero tangential component of the velocity x_t . Once again this is confirmed by our numerical experiment, as can be seen from the plot of $\|D_t x^{m+1} \cdot \theta^m\|_{0,h}$ in Figure 10, which seems to be monotonically increasing. We remark that we repeated the simulations in Figures 9 and 10 with finer discretization parameters and obtained visually indistinguishable results. Hence, we are confident that the displayed evolution provides numerical evidence that the two PDEs (1.4a) and (1.5), with the initial conditions (1.4b), parameterize different curve evolutions.

REFERENCES

- [1] J. W. BARRETT, H. GARCKE, AND R. NÜRNBERG, *Parametric finite element approximations of curvature driven interface evolutions*, in Geometric Partial Differential Equations. Part I, Handb. Numer. Anal. 21, A. Bonito and R. H. Nochetto, eds., Elsevier, Amsterdam, 2020, pp. 275–423.
- [2] K. DECKELNICK, G. DZIUK, AND C. M. ELLIOTT, *Computation of geometric partial differential equations and mean curvature flow*, Acta Numer., 14 (2005), pp. 139–232.
- [3] G. DONG, M. HINTERMUELLER, AND Y. ZHANG, *A class of second-order geometric quasilinear hyperbolic PDEs and their application in imaging*, SIAM J. Imaging Sci., 14 (2021), pp. 645–688.
- [4] G. DZIUK, *Discrete anisotropic curve shortening flow*, SIAM J. Numer. Anal., 36 (1999), pp. 1808–1830.
- [5] K. ECKER, *Regularity Theory for Mean Curvature Flow*, Birkhäuser, Boston, 2004.
- [6] C. M. ELLIOTT AND H. GARCKE, *Existence results for diffusive surface motion laws*, Adv. Math. Sci. Appl., 7 (1997), pp. 465–488.
- [7] M. GAGE AND R. S. HAMILTON, *The heat equation shrinking convex plane curves*, J. Differential Geom., 23 (1986), pp. 69–96.
- [8] Y. GIGA, *Surface Evolution Equations*, Monogr. Math. 99, Birkhäuser, Basel, 2006.
- [9] E. GINDER AND K. SVADLENKA, *Wave-type threshold dynamics and the hyperbolic mean curvature flow*, Jpn. J. Ind. Appl. Math., 33 (2016), pp. 501–523.
- [10] C. GROSSMANN AND H.-G. ROOS, *Numerical Treatment of Partial Differential Equations*, Universitext, Springer, Berlin, 2007.
- [11] M. E. GURTIN AND P. PODIO-GUIDUGLI, *A hyperbolic theory for the evolution of plane curves*, SIAM J. Math. Anal., 22 (1991), pp. 575–586.
- [12] C.-L. HE, S. HUANG, AND X. XING, *Self-similar solutions to the hyperbolic mean curvature flow*, Acta Math. Sci. Ser. B (Engl. Ed.), 37 (2017), pp. 657–667.
- [13] C.-L. HE, D.-X. KONG, AND K. LIU, *Hyperbolic mean curvature flow*, J. Differential Equations, 246 (2009), pp. 373–390.
- [14] G. HUISKEN, *Flow by mean curvature of convex surfaces into spheres*, J. Differential Geom., 20 (1984), pp. 237–266.
- [15] D. KONG, K. LIU, AND Z. WANG, *Hyperbolic mean curvature flow: Evolution of plane curves*, Acta Math. Sci. Ser. B (Engl. Ed.), 29 (2009), pp. 493–514.
- [16] D.-X. KONG AND Z.-G. WANG, *Formation of singularities in the motion of plane curves under hyperbolic mean curvature flow*, J. Differential Equations, 247 (2009), pp. 1694–1719.
- [17] P. G. LEFLOCH AND K. SMOCZYK, *The hyperbolic mean curvature flow*, J. Math. Pures Appl. (9), 90 (2008), pp. 591–614.
- [18] C. MANTEGAZZA, *Lecture Notes on Mean Curvature Flow*, Progr. Math. 290, Birkhäuser/Springer Basel AG, Basel, 2011.
- [19] W. W. MULLINS, *Theory of thermal grooving*, J. Appl. Phys., 28 (1957), pp. 333–339.
- [20] H. G. ROTSTEIN, S. BRANDON, AND A. NOVICK-COHEN, *Hyperbolic flow by mean curvature*, J. Cryst. Growth, 198–199 (1999), pp. 1256–1261.

- [21] J. E. TAYLOR AND J. W. CAHN, *Linking anisotropic sharp and diffuse surface motion laws via gradient flows*, J. Statist. Phys., 77 (1994), pp. 183–197.
- [22] T. J. WILLMORE, *Riemannian Geometry*, Oxford Science Publications, The Clarendon Press, Oxford University Press, New York, 1993.
- [23] S.-T. YAU, *Review of geometry and analysis*, in Mathematics: Frontiers and Perspectives, AMS, Providence, RI, 2000, pp. 353–401.